Running head: Environmental variability and density dependence in Taylor's law

Title:

Environmental variability and density dependence in the temporal Taylor's law

Authors:

Takashi Saitoh[1,*], Joel E. Cohen[2]

Affiliations:

[1] Field Science Center, Hokkaido University, North-11, West-10, Sapporo 060-0811, Japan

[2] Laboratory of Populations, The Rockefeller University and Columbia University, 1230 York Ave., Box 20, New York, NY 10065-6399, USA; also Earth Institute and Department of Statistics, Columbia University, and Department of Statistics, University of Chicago

* Corresponding author:

Takashi Saitoh

Field Science Center, Hokkaido University, North-11, West-10, Sapporo 060-0811, Japan

Email: tsaitoh@fsc.hokudai.ac.jp

Abstract

Taylor's law (TL) is an empirical rule describing the approximate relationship between the variance and the mean of population density: $\log_{10}(\text{variance}) \approx \log_{10}(a) + b \times \log_{10}(\text{mean})$. Although TL has been verified in various ecological systems, essential questions remain unanswered. Why is TL so widely observed? What mechanisms or processes generate TL? Why do most observed slopes b fall in the limited range $1 < b < 2$? Density-dependent movement of individuals among populations has been proposed as a mechanism that leads to TL with slopes $1 < b < 2$. We used the Gompertz model (a second-order autoregressive model of the logarithm of population density) to analyze the temporal TL of gray-sided vole populations. Our extensive simulations using various combinations of model parameters for environmental variability and density dependence demonstrated that sustainable populations could obey TL in the absence of density-dependent movement among populations, and identified the parameter combinations that produced slopes $1 < b < 2$. When environmental variability was low and density dependence was intermediate, simulated data sets showed higher probabilities for $1 < b < 2$, but the probability was not very high. In general, slopes became steeper (b increased) as environmental variability increased and as density dependence coefficients decreased. In the Gompertz model, both environmental variability and density dependence cause population density to vary, and on the logarithmic scale of population density, those effects are symmetric above and below the equilibrium density. However, effects of the variability are higher above the equilibrium density on the natural scale of population density, and thus the mean of population density increases with increasing population variability. Therefore, the temporal TL can be formed when population density is measured in the natural scale. In sustainable populations well described by the Gompertz model, the slope b can be determined by the interplay of environmental variability and density dependence.

Keywords:

Autoregressive time series

Density dependence

Environmental variability

Rodents

Slope

Taylor's law

1. Introduction

Taylor's law (TL, Taylor 1961) is an empirical rule describing the approximate relationship between the variance and the mean of population density. It has been widely verified in various ecological systems (Taylor 1986) and many other fields (Eisler et al. 2008, Tippett and Cohen 2016). TL asserts that the variance is approximately a power-law function of the mean: variance = $a \times (\text{mean})^b$, $a > 0$. It is usually rewritten:

$$\log_{10}(\text{variance}) = \log_{10}(a) + b \times \log_{10}(\text{mean}). \quad \text{(Eq. 1)}$$

Neither of these equations specifies the deviations from an exact relationship, i.e., the error term in TL.

The mean and the variance of population density can be calculated temporally and spatially. In the temporal TL, the mean and the variance are calculated over observations of population density at different times in a given location, while in the spatial TL, the mean and the variance are calculated over observations of population density in different spatial locations at a given time. The temporal mean of population density may depend primarily on habitat quality, while the temporal variance of population density may be produced primarily by population dynamics in interaction with environmental variable factors, which broadly include abiotic (e.g., climatic, chemical, physical) and biotic (e.g., trophic, parasitic, allelopathic) effects on a given species. This study investigated the relative contributions of population dynamics and environmental variability in shaping the form and parameters of the temporal variance-mean relationship.

Many theoretical models and interpretations of TL have been proposed, but none has gained widespread acceptance. Essential questions remain unanswered. Why is TL so widely observed? What mechanisms or processes generate TL? Why do most observed slopes satisfy $1 < b < 2$? Although combined empirical and theoretical studies should be conducted to answer these questions, many previous empirical studies have verified TL without testing the

details of any model that leads to TL, while theoretical models that lead to TL have often lacked detailed empirical verification of the processes assumed (see reviews by Taylor 1986, Kendal 2004, Eisler et al. 2008, but as exceptions see Cohen et al. 2013; Linnerud et al. 2013).

We found previously that the population density of the gray-sided vole, *Myodes rufocanus* (Sundevall, 1846), in Hokkaido satisfied the temporal TL, and the estimated slope 1.613 was in $1 < b < 2$ (Cohen and Saitoh 2016). Moreover, Cohen and Saitoh (2016) showed that the densities of different vole populations were not independent. The Gompertz model, which describes well the dynamics of the logarithm of population density of those populations (Royama 1977, 1992; Stenseth 1999; Stenseth et al. 2003), generated time series of density on the original scale of measurement that satisfied the form of temporal TL, but, under the assumption that different populations were independent, the slope $b \approx 2.699$ of the simulated TL was significantly steeper than the slope of the empirical populations. We attributed this discrepancy to the assumed independence of simulated time series.

In contrast to the independent simulated time series, empirical populations may inhabit habitats of varying quality, may be subject to correlated environmental influences (the "Moran effect"), and may experience density dependent movements from a higher-quality habitat to a lower-quality habitat. Density-dependent movement reduces the temporal mean and variance of populations in higher-quality habitats, while it enhances the temporal mean and variance of populations in lower-quality habitats. Therefore, density-dependent movements could lower the temporal slope of TL, as Taylor and Taylor (1977) and Perry (1988) suggested. Synchrony of populations produced by the Moran effect could also lower the slopes of the spatial TL (Reuman et al. 2017).

Density-dependent movements, however, seem unrealistic for the studied vole populations, because the distance between the studied vole populations is far beyond the

movement ability of individuals of the gray-sided vole. The mean geographic distance between the observed populations was 8.4 km, while most natal dispersals of individuals are recorded within several hundred meters (Ishibashi and Saitoh 2008), although some long-distance movements of up to several kilometers have been reported in some arvicoline rodent populations, which are highly variable (see Le Galliard et al. 2012 for a review). Therefore, we shall test whether TL can be formed, with realistic values of the slope parameter *b*, even in the absence of demographically significant migration.

Here we report detailed simulations of the temporal TL for the empirical populations of the gray-sided vole using the Gompertz model with extensive combinations of model parameters. These results will shed light on the above general questions about TL in this situation.

Modelling of population dynamics is a powerful approach to simulating observed populations, analyzing effects of model parameters, and considering underlying mechanisms of the temporal TL. Anderson et al. (1982) proposed a Markovian population model where chance demographic events could lead to the temporal TL by the adjustment of the relative rates governing birth, death, immigration, and emigration. Perry (1988) demonstrated that models based on density-dependent movement could yield the temporal TL. Hanski and Woiwod (1993) simulated populations where the intrinsic growth rate of populations was subjected to a random component; these simulated populations approximated the temporal TL. All of these attempts, however, relied upon arbitrary approximations, transformations or constraints to achieve the goal (Kendal 2004). In addition, the models of population dynamics used by those studies were not tested to evaluate whether they could describe empirical populations well, and some models were unrealistic. For example, Anderson et al. (1982) assumed a potentially infinite increase of population density, and Perry (1988) assumed

density-dependent movement that is unrealistic, at least for the studied populations of the gray-sided vole.

Linnerud et al. (2013) analyzed density dependence and stochastic effects on the temporal TL using empirical data on avian populations and modified logistic models. They claimed that slopes of the temporal TL were influenced by interspecific variation in life history parameters (adult survival and clutch size). However, their examined parameter space of population dynamics was limited. In contrast, Royama (1977, 1992) examined the relationship between the density-dependence coefficients and the population dynamics of the Gompertz model (details below) and identified the parameter space of density-dependence coefficients where populations are sustainable (mathematically speaking, where the second-order autoregressive model is stationary and ergodic). Therefore, we can thoroughly analyze effects of density dependence on the temporal TL for sustainable populations using the Gompertz model with fewer arbitrary approximations or assumptions.

Here we will show, first, that the variability of population density derives from both environmental variability and density dependence. Second, by extensive analyses of environmental variability and density-dependence coefficients without assuming density-dependent movements or environmentally caused synchrony, we will show that sustainable populations satisfy the temporal TL and will identify parameter combinations that are more likely to produce slopes $1 < b < 2$. Further, we will show that a driving force of the temporal TL formation is population variability but not the variation of the equilibrium density.

2. Materials and methods

2.1. Study design and data

Hokkaido is the northernmost island of Japan (78,073 km^2). The gray-sided vole, *Myodes rufocanus* (Sundevall, 1846), is the commonest species of rodents on this island (Kaneko et

al. 1998). A systematic survey of rodent populations has been carried out in Hokkaido by Forestry Agency of Japanese Government. The geography of Hokkaido and the data collection were described previously (Saitoh et al. 1997, 1998; Stenseth et al. 2003). We analyzed the same data set of the gray-sided vole as Cohen and Saitoh (2016): $N = 85$ populations in different locations covering $T = 31$ years (1962–1992). Population density was defined as the number of voles per 150 trap-nights, because 50 snap traps for three consecutive nights on a 0.5 ha survey plot was a standard unit of the rodent survey.

The Bayesian method was applied to the estimation of population density for each year and location based on a state-space model by using WinBUGS version 1.4.3 (Spiegelhalter et al. 2003, http://www.mrc-bsu.cam.ac.uk/software/bugs/). In our previous study (Cohen and Saitoh 2016), population density was estimated assuming that the number of voles caught increased in proportion to trapping effort. However, there were some limitations imposed by the trapping method. Because the basic unit of trapping was 150 trap-nights, the number of catches could not exceed 150 per unit. New codes for WinBUGS were developed taking the constraints of trapping into consideration. In addition, non-target species of rodents (*Apodemus argenteus, A. speciosus,* and other minor species) than the target species (*Myodes rufocanus*) provided some small proportion of caught rodents, although the target species dominated other species (Saitoh and Nakatsu 1997). Traps occupied by other species should not be considered effective traps. Therefore we subtracted the number of catches with non-target species from the number of trap-nights. The new codes for WinBUGS are available as Appendix B. The raw counts of voles trapped, the trapping effort (the total number of trap-nights, excluding traps occupied by non-target species), and the resulting Bayes population estimates are available in a spreadsheet file as Appendices H–K.

Although we used the natural logarithm of the number of individual voles trapped per unit of trapping effort (one trap-night) for the analysis by WinBUGS, we transformed the estimates back to the original scale of measurement, the number of voles captured per 150 trap-nights (the basic unit of trapping), for the following analyses of TL.

2.2. Temporal Taylor's law

The mean and the variance were calculated over observations of population density at different times in a given location, and one data point [$\log_{10}$(temporal mean), $\log_{10}$(temporal variance)] was plotted for each location. Ordinary least-squares regression (OLS) was used to test the temporal TL, by fitting Eq. 1 to $\log_{10}$(temporal mean) and $\log_{10}$(temporal variance) of the vole populations and simulated time series.

2.3. Gompertz model

We used the second-order autoregressive model (the Gompertz model; Eq. 2) to describe population dynamics of the gray-sided vole. In this model, for each population j = 1,…, 85, $x_{t,j}$ was the natural logarithm of Bayesian estimate of the observed density ($N_{t,j}$) in year t = 1962,…,1992; $\overline{x_j}$ was the temporal mean of $x_{t,j}$ in population j, and $x_{t,j} - \overline{x_j}$ was the centered time series on the logarithmic scale in population j. The Gompertz model supposes that

$$x_{t,j} - \overline{x_j} = (1 + a_{1,j})(x_{t-1,j} - \overline{x_j}) + a_{2,j}(x_{t-2,j} - \overline{x_j}) + e_{t,j} , \qquad \text{(Eq. 2)}$$

where for each population j, the parameters $a_{1,j}$ and $a_{2,j}$ are the coefficient of density dependence for a 1-year lag and for a 2-year lag, respectively. The error term $e_{t,j}$ represents density-independent effects (environmental variability) modeled as random numbers from a normal distribution with mean 0 and a variance SD_j^2. Fitting the Gompertz model (Eq. 2) to

the centered time series $x_{t,j} - \overline{x_j}$ yielded Bayesian estimates of $a_{1,j}$, $a_{2,j}$, and SD_j (see the WinBUGS codes in Appendix B for details).

Stenseth et al. (1996) assessed the order of the autoregressive model by fitting the models to the gray-sided vole populations in Hokkaido and demonstrated that the second order is parsimonious; in 93% of the populations second or lower order was selected as the best model.

Population density depends on habitat quality. In a higher-quality habitat, a population would be expected to show a higher mean population density. When an equilibrium exists, it can be modeled as the mean density $\overline{x_j}$ in the Gompertz model (Fig. 1A), which equals the natural logarithm of the geometric mean density on the original scale of density. A population may stay at its equilibrium density if no perturbation affects its population density. However, most environments are variable, and a population may be forced to move from the equilibrium by environmental variability (arrows away from the equilibrium). A sustainable population never continues moving further from the equilibrium, but rather displays a tendency to return to the equilibrium (arrows toward the equilibrium). Such return tendency is defined as density dependence. Therefore, apart from the effects of dispersal of individuals from and to other populations, which we take as zero in the present study, a population is limited by the equilibrium related to habitat quality, is varied by environmental variability, and is regulated by density dependence in general, although effects of density dependence are not simple and can enhance the variability of population dynamics, combined with environmental variability.

Royama (1977, 1992) used standard results from the statistical theory of second-order autoregressive time series (e.g., Box and Jenkins 1970, pp. 58-63) to analyze the relationship between fluctuation patterns of population dynamics and the density-dependence coefficients a_1 and a_2 (Fig. 1B). Inside the triangle of Fig. 1B, assuming $SD_j = 0$ (hence no environmental

variability), the dynamics is either point stability or damped fluctuations. Fluctuations will persist if any stochasticity exists ($SD_j > 0$). In general, less variable populations show parameters in the upper-right part (I) of the triangle (Bjørnstad et al. 1995). Appendix G gives some new mathematical analysis of Taylor's law for second-order autoregressive time series.

2.4. Simulations

We carried out five simulations, called Fundamental simulation I, Fundamental simulation II, Synchronized simulation, Parameter combination simulation I, and Parameter combination simulation II. We distinguish the observed values $x_{t,j}$ in Eq. (2) from the simulated values $y_{t,j}$ in Eq. 3:

$$y_{t,j} = (1 + a_{1,j})(y_{t\text{-}1,j} - \overline{x_j}) + a_{2,j}(y_{t\text{-}2,j} - \overline{x_j}) + \overline{x_j} + e_{t,j}. \quad \text{(Eq. 3)}$$

The initial two observed log-transformed values $x_{1,j}$, $x_{2,j}$ were used for the first two values ($y_{1,j} = x_{1,j}$ and $y_{2,j} = x_{2,j}$) of each simulated population. The state variable in all simulations was the centered log-transformed population density $y_{t,j} - \overline{x_j}$.

2.4.1. Fundamental simulations I and II

In the Fundamental simulation I, we used the population-specific estimates of $a_{1,j}$ and $a_{2,j}$ and SD_j corresponding to the 85 observed populations and generated 85 time series spanning 31 years ($y_{t,j}$). The environmental variability $e_{t,j}$ was assumed to be uncorrelated between different years t and between any two populations. For each population j separately, a primary $e_{t,j}$ was given as independent and identically distributed normal random numbers with mean 0 and variance SD_j^2, [$\mathcal{N}_{tj}(0, SD_j^2)$]. Since the length of $e_{t,j}$ was limited to 31 (years), the mean and the SD of simulated environmental variability $e_{t,j}$ were accidentally higher or lower than expected. To adjust the mean and the SD, the primary $e_{t,j}$ was then adjusted by the following equation: the adjusted $e_{t,j}$ = [the primary $e_{t,j}$ – temporal mean(the

primary $e_{\cdot,j}$)] × [SD_j / temporal SD(the primary $e_{\cdot,j}$)]. The Fundamental simulations I and II used the adjusted $e_{t,j}$ as the simulated environmental variability.

One thousand data sets, each of which consisted of the 85 simulated time series, were generated. The generated values were then transformed back by exponentiation to the original scale of population density, and temporal means and variances were computed on the original scale of population density for tests of the temporal TL using the OLS regression.

Some unrealistically high values for population densities were observed in simulated time series of the Fundamental simulation I. A small number of simulated values (0.52%) were higher than the maximum of density estimates (–0.1955 on the $\log_e$ scale, equivalent to 123.4 per 150 trap-nights in the original scale) for the observed populations. The lowest simulated value was very close to that for the observed populations. Since those unrealistically high values caused higher variances of population density in simulated time series, an upper limit was set in the Fundamental simulation II. When a simulated value exceeded –0.1955, that value was replaced with –0.1955. Other procedures of the simulation were the same as those of the Fundamental simulation I. The temporal TL was tested for each of 1,000 simulations of 85 populations using OLS regression.

2.4.2. Synchronized simulations

To synchronize e_t, we first generated a fixed "baseline error" time series $e_{t,0}$ of 31 independent and identically distributed normal random numbers with mean 0 and variance 1. Then we generated 85 correlated time series $e_{t,j}$, j = 1, …, 85, of length 31 years (t = 1, …, 31), using the formula: primary $e_{t,j} = \rho \times e_{t,0} + (1 - \rho)^{1/2} \times \mathcal{N}_{t,j}(0, SD_j^2)$, where $\mathcal{N}_{t,j}(0, SD_j^2)$ are independent and identically distributed normal random numbers with mean 0 and variance SD_j^2, and the primary $e_{t,j}$ was rescaled as in the Fundamental simulations I and II: the adjusted $e_{t,j}$ = [the primary $e_{t,j}$ – temporal mean(the primary $e_{\cdot,j}$)] × [SD_j / temporal SD(the primary $e_{\cdot,j}$)]. We tuned ρ to 0.69 so that the average correlation among simulated time series

(the range of the average correlations: 0.216 – 0.294) closely approximated the average correlation among the observed populations (average correlation = 0.277).

Other procedures of the simulation were the same as those of the Fundamental simulation II. One thousand simulations of the 85 time series were generated. The generated values were then transformed back to the original scale of population density, and temporal means and variances were computed on the original scale of population density for tests of the temporal TL using the OLS regression.

2.4.3. Parameter combination simulation I

We explored which combinations of the model parameters would be more likely to generate prevailing slopes ($1 < b < 2$) by using the observed mean densities ($\bar{x}_j$) and various combinations of model parameters in the Fundamental simulation I (Eq. 3). To each simulated set of 85 time series spanning 31 years ($y_{t,j}$), a specific set of the parameters (a_1, a_2, and SD) was given in Parameter combination simulation I: $1 + a_1$ ranged from –1.95 to 1.95 with the increment of 0.05, a_2 ranged from –0.975 to 0.975 with the increment of 0.05, and SD ranged from 0.05 to 2 with the increment of 0.05. The combinations of $1 + a_1$ and a_2 were restricted to the range in which time series were sustainable, i.e., 1,600 combinations such that each point ($1 + a_1$, a_2) fell within the triangle in Fig. 1B. Since simulations were carried out with 40 different SDs for each combination of $1 + a_1$ and a_2, 64,000 data sets of 31×85 $y_{t,j}$ were generated. For each data set, OLS regression was used to estimate the slope of the temporal TL.

2.4.4. Parameter combination simulation II

In all the above simulation analyses, an observed mean density was given as the equilibrium density to each simulated time series. To extend the generality of those analyses, various hypothetical mean densities m_j were given as an equilibrium density to the Gompertz model in Parameter combination simulation II:

$$k_{t,j} = (1 + a_{1,j})(k_{t-1,j} - m_j) + a_{2,j}(k_{t-2,j} - m_j) + m_j + e_{t,j}, \quad \text{(Eq. 4)}$$

where m_j was an equilibrium density of each time series. Here $e_{t,j}$ was drawn from a normal distribution with mean 0 and variance 1. The following 16 values were given as standard mean densities per 150 trap-nights in the original scale for m_j: 2, 4, 6, 8, 10, 12, 14, 16, 18, 20, 50, 100, 200, 300, 400, and 500. To make the equilibrium densities vary in the simulations, a normally distributed random number with mean = a standard mean density and $SD^2 = 1$ in the logarithmic scale was given to each simulated time series as an equilibrium density. The 1,600 combinations of $1 + a_1$ and a_2 were the same as above, while the range of SD was limited between 0.05 and 1 (20 cases), to reduce calculation load. Then 85 time series spanning 31 years ($k_{t,j}$) were generated for each parameter combination, and 512,000 = 1600 × 16 × 20 sets of 31 × 85 $k_{t,j}$ were obtained in total. For each such set of simulated time series, OLS regression was used to estimate the slope of the temporal TL.

2.5. Cause and factors of Taylor's law

Simulated time series are defined by three parameters (a_1, a_2, and SD) and the equilibrium density (m). We examined how the variance and the mean of density of the simulated times series were related to those variables through multiple regression analyses with slope b of TL as a response variable and with the parameters and the equilibrium density as explanatory variables. All regressions were computed using function "lm" in R version 3.4.3. The critical value for statistical significance was always $P = 0.05$. We made no corrections for simultaneous inference (i.e., multiple tests of a null hypothesis of no effect), hence approximately 5% of our apparently "significant" results could have arisen by chance alone.

3. Results

3.1. Temporal Taylor's laws

In comparison with our previous study, densities estimated in this study were higher than those in Cohen & Saitoh (2016) in general (Appendix A). Although both the mean and the variance of density estimates were higher in this study, the variance increased by more than the mean. Therefore, the slope of the temporal TL, Eq. 1, became steeper (Fig. 2A): $\log_{10}$(variance) = 0.063 (± SE 0.133) + 1.943 (± SE 0.143) × $\log_{10}$(mean) (t = 13.576, $P < 2.0 \times 10^{-16}$, Adjusted R^2 = 0.686), while Cohen & Saitoh (2016) estimated $\log_{10}$(variance) = 0.217 (± 0.124) + 1.613 (± 0.141) × $\log_{10}$(mean). The lower and upper limit of the 95% confidence interval of the current estimate of the slope was 1.659 and 2.228, respectively. Because a quadratic regression revealed no statistically significant evidence of nonlinearity (Appendix A), we focus on the linear relationship henceforth. The 3,570 pairs (3,570 = 85 × 84/2) of vole populations had correlation coefficients of population density that ranged from a low of –0.359 to a high of 0.886, with a mean correlation of 0.277 ± 0.211 (SD).

The temporal TL described all 1,000 data sets generated by the Fundamental simulation I reasonably well (Adjusted R^2: 0.542 – 0.824). Their slopes ranged between 2.145 and 3.009 (mean = 2.618, SD = 0.144, Fig. 2B). SEs of the slopes ranged between 0.145 and 0.233, and all SEs were smaller than 10% of the estimates of the slopes. A very small number of slopes (7, 0.7%) were lower than the upper limit of the 95% confidence interval of the slope estimate for the observed populations. This means that the slopes of Fundamental Simulation I were mostly too high when compared with the slope estimated from observations. The overall mean of mean pairwise correlation coefficients of population density for 1,000 data sets was 0.007 ± 0.003 (SD), which was consistent with the independence between populations assumed in Fundamental simulation I.

The temporal TL described all 1,000 data sets generated by the Fundamental simulation II reasonably well (Adjusted R^2: 0.485 – 0.767). Their slopes ranged between

1.899 and 2.568 (mean = 2.278, SD = 0.107, Fig. 2C). SEs of the slopes ranged between 0.146 and 0.232, and 95% of SEs were smaller than 10% of the estimates of the slopes. A considerable number of slopes (320, 32.0%) fell within the 95% confidence interval of the slope estimate for the observed populations. This means that the slopes of Fundamental Simulation II were closer to the slope estimated from observations than were the slopes of Fundamental Simulation I, but more than two-thirds of the slopes were still too high. The overall mean of mean pairwise correlation coefficients of population density for 1,000 data sets was 0.007 ± 0.003 (SD), not different from that in Fundamental simulation I.

The temporal TL described all 1,000 Synchronized simulations reasonably well (Adjusted R^2: 0.424 – 0.766). Their slopes ranged between 1.756 and 2.642 (mean = 2.276, SD = 0.112). SEs of the slopes ranged between 0.147 and 0.223, and 95% of SEs were smaller than 10% of the estimates of the slopes. A similar proportion of slopes (32.8%) were included in the 95% confidence interval of the slope estimate for the observed populations, in comparison with those in the Fundamental simulation II. This means that more than two-thirds of the slopes were still too high. The mean of pairwise correlation coefficients of population density ranged between 0.216 and 0.294 (the overall mean = 0.277, n = 1000), which was close to the observed one (0.277). The SD of the pairwise correlations of the simulated populations ranged between 0.215 and 0.238, and they were also close to that of the observed populations (0.211).

The slopes did not differ between data sets from Fundamental simulation II (mean = 2.278) and the Synchronized simulation (mean = 2.276, Welch two sample t-test, t = 0.282, P = 0.778), the variance was also similar between Fundamental simulation II (0.011) and the Synchronized simulation (0.012, F-test, F = 0.909, P = 0.131). No statistically significant difference in the proportion of the slopes that were included in the 95% confidence interval of

the slope estimate for the observed populations was detected between the Fundamental simulation II and the Synchronized simulation (Fisher's exact test, $P = 0.738$).

3.2. Conditions for slopes $1 < b < 2$

3.2.1. Parameter combination simulation I

We explored conditions of environmental variability and density dependence that produced slopes $1 < b < 2$, using the 64,000 data sets in Parameter combination simulation I.

Slopes from the 64,000 data sets ranged between 0.539 and 3.529 (mean = 2.294, SD = 0.247, Fig. 3A). SEs of the slopes ranged between 0.001 and 0.348, and 95% of SEs were smaller than 10% of the estimates of the slopes. Few of the time series (0.05%) showed slopes $b \leq 1$, and 7,035 time series (10.99%) showed slopes $1 < b < 2$. Most times series (88.96%) showed slopes exceeding 2.

Model parameters that produced slopes $1 < b < 2$ were distributed in a limited region (Fig. 3; Appendix D). When SD was low, simulated time series showed higher probabilities that their slopes fell in the prevailing range. The highest probability (0.462) was observed when SD = 0.10, and the probabilities for values of SD from 0.05 to 0.20 were higher than 0.4 (Fig. 3D). That probability drastically decreased as SD increased from SD = 0.25 and fell below 0.01 as SD increased from SD = 0.90 to 2.00. The number of data sets with $1 < b < 2$ amounted to 7,005 for values of SD from 0.05 to 0.95, which was 99.6% of the total number of the data sets with the prevailing slopes. In the range of SD between 1 and 2, most data sets (99.9%) showed slopes steeper than 2; the mean of the slopes was 2.362 with variance = 0.029. Data sets with lower SD from 0.05 to 0.95 showed a lower mean of slopes (2.219) with a higher variance (0.085; Welch two sample *t*-test for the mean, $t = 74.351$, $P < 2 \times 10^{-16}$, *F*-test for the variance, $F = 2.899$, $P < 2 \times 10^{-16}$).

Since the variation of slopes was small in the range of SD between 1 and 2, we focused on simulated data sets with lower SD between 0.05 and 0.95. Density dependence coefficients ($1 + a_1$ and a_2) showed a roughly similar pattern for the probabilities that TL slopes fell in $1 < b < 2$. A clear peak was found in the middle of the range (Figs. 3B and 3C). The highest probability (0.420) was observed when $1 + a_1 = -0.1$, while it was 0.424 when a_2 was 0.175.

A multiple regression analysis focused on these simulated data sets with SD between 0.05 and 0.95. Slope b was considered as a response variable, while density dependence coefficients ($1 + a_1$ and a_2), environmental variability (SD) and their pairwise products were used as explanatory variables (Table 1). All these explanatory variables and their products contributed significantly to explain the variation of the slope, and the full model showed a moderate goodness of fit ($R^2 = 0.480$). Summarizing the results of this analysis, slopes became steeper with the increase of SD and with the decrease of a_1 and a_2 (Appendix E).

For each combination of $1 + a_1$ and a_2 and for SD between 0.05 and 0.95, the probability that slopes fell in $1 < b < 2$ was higher near the center of the triangle (Fig. 4), extending toward the upper-right. Most observed populations of the gray-sided vole had values of $1 + a_1$ and a_2 in this high-probability region.

3.2.2. Parameter combination simulation II

The effects of equilibrium densities on the temporal TL were examined in Parameter combination simulation II. Slopes of the 512,000 simulated data sets ranged between 1.680 and 2.556. SEs of the slopes ranged between 0.003 and 0.147, and all SEs were smaller than 10% of the estimates of the slopes. The number of the data sets with $1 < b < 2$ was 123,494 (24.1%).

A multiple regression analysis, in which slope b was used as a response variable and equilibrium densities (m), density dependence coefficients (a_1 and a_2), environmental

variability (SD) and their pairwise products were used as explanatory variables, showed a minor contribution of equilibrium densities (Table 2; Appendix F). Effects of equilibrium densities and related products were not significant, and the selected model consisted of a_1, a_2, SD and their pairwise products, without equilibrium densities and related products.

4. Discussion

4.1. The Gompertz model

The Gompertz model has been known as a model that describes well the dynamics of some populations, including the populations of gray-sided voles in this study (Royama 1977, 1992; Stenseth 1999; Stenseth et al. 1996, 2003). The Gompertz model has frequently been used to characterize rodent populations and compare their population dynamics among localities or periods (e.g., Stenseth 1999; Cornulier et al. 2013).

Fundamental simulations I reproduced the form of the temporal TL, but not the empirical slope (Fig. 2B). For some values of the simulated mean, Fundamental simulation I gave an unusual simulated variance that appeared to be far higher than the observed variance associated with the observed mean that matched the simulated mean. The higher variances were attributed to some unusually high values for population densities in Fundamental simulation I. Unrealistic values of density, which exceeded the maximum of density estimates per 150 trap-nights in the original scale (123.4) for the observed populations, were observed in 0.52% of simulated densities. Therefore, an upper limit was introduced for simulated densities in the Fundamental simulation II: a simulated density that exceeded the maximum density was replaced with the maximum density. As a result, 32.0% of slopes in 1,000 simulated data sets were included in the 95% confidence interval of slope estimates for the observed populations (Fig. 2C). The generation of unrealistically high values is a methodological limitation of this study.

Slopes of the temporal TL in the Synchronized simulations were very similar to the slopes of the temporal TL in the Fundamental simulation II. The mean and the variance of slopes were similar (2.278 and 0.011 for the Fundamental simulation II, 2.276 and 0.012 for the Synchronized simulation), and the percentage of slopes that were included in the 95% confidence interval of slope estimates for the observed populations differed little (32.0% for the Fundamental simulation II, 32.8% for the Synchronized simulation). Therefore, synchrony may not have major effects on the temporal TL of the studied populations.

The temporal TL can arise from the combination of environmental variability and density dependence. It was unnecessary to assume density dependent movements among populations for the studied populations at least. Such density dependent movements among populations have been considered sufficient conditions to produce the prevailing slopes of TL ($1 < b < 2$) in earlier studies (Taylor and Taylor 1977; Hanski 1982; Perry 1988). The mean geographic distance between the observed populations was 8.4 km (range: 3.6–22.7 km). The mean home range length of the gray-sided vole in Hokkaido is 16.3 m (range: 10–40) for females and 32.7 m (10 – 65) for males, and the longest natal dispersal distance was recorded in young males ($n = 46$) with median 103.5 m, inter-quartile range 56.9–135.0 m (Ishibashi and Saitoh 2008). It is, therefore, implausible to assume that gray-sided voles frequently moved between the observed populations (see also Bjørnstad et al. 1999). Consequently we argue that the observed temporal TL may be formed by density dependence, environmental variability, and their interactive products.

However, this study does not deny the effects of density dependent movements on slopes of the temporal TL in other ecological systems. Some reports showed density dependent dispersal and long distance reaching several kilo meters in arvicoline rodents, although the effects of density on dispersal are not simple; more reports show negative density dependent movements than show positive density dependent movements (Le Galliard

et al. 2011). In addition, mobile predators that travel long distance influence features of dynamics in populations and may make a correlation among populations that do not directly interact by movements (e.g., Ims and Andressen 2000). As a result, they could moderate or exaggerate the variance of population density in the absence of mobile predators. Comparative studies covering various systems are needed to test these effects.

4.2. Cause and processes of the temporal TL formation

By giving the Gompertz model various combinations of model parameters, we explored causes and processes of temporal TL formation.

The multiple regression analysis based on Parameter combination simulation I, in which the slope was a response variable and density dependence coefficients (a_1 and a_2), environmental variability (SD) and their products were explanatory variables, showed that those variables significantly contributed to explaining the variation of the slope, and that slopes became steeper with the increase of SD and with the decrease of a_1 and a_2 (Table 1). The effects of another variable included in the Gompertz model, equilibrium density, were tested in Parameter combination simulation II, in which equilibrium densities ranged between 2 and 500 per 150 trap-nights in the natural scale. Although all sets of time series satisfied the form of the temporal TL, equilibrium densities had no significant effects on slopes (Table 2). These results indicate that environmental variability (SD), density dependence coefficients (a_1 and a_2), and their products sufficed to explain the slopes in the temporal TL.

A closed population (without significant dispersal in or out) is limited by habitat quality (limitation), is perturbed by environmental variability, and is regulated by density dependence (regulation) in general (Fig. 1A). Environmental variability is a major source for the variance of population density in our model, although effects of density dependence also contribute to the variability of population density. Environmental variability, represented by

the error term (e_t) in our model, moves population density away from the equilibrium density. Since the error term is modeled by a normal distribution with mean equal to 0 and a variance SD^2, environmental variability provides symmetric effects above and below the equilibrium density on the log scale of density (Fig. 1A). Therefore, higher environmental variability generates higher variances of population density x_t on the log scale of density without altering the mean density ($\bar{x}$) on the log scale. However, the effects of environmental variability are asymmetric above and below the equilibrium density in the original scale of population density (N_t). The effects of environmental variability are unlimited above the equilibrium density but are limited below the equilibrium density because N_t does not take a negative value. Therefore, higher environmental variability generates higher variability of populations and higher mean density ($\overline{N}$) on the natural scale of population density, and the temporal TL can be formed on the natural scale of population density. Our simulated environmental variability is normally distributed on the logarithmic scale or lognormally distributed on the original scale of density. It is well known that the mean of a lognormal random variable increases with any increase, on the logarithmic scale, in either its mean or its variance or both. The Supplementary Discussion of Tippett and Cohen (2016) describes several ways the lognormal distribution can generate TL with different slopes.

Density dependence together with the interaction with environmental variability also influences the variability of populations and may contribute to the temporal TL formation through a process similar to environmental variability. In our model, equilibrium densities on the log scale of density do not affect the temporal variance of density, although equilibrium density influences the mean density on the original scale of density.

Taylor's law asserts that the variance in the population density is a power-law function of its mean population density. It implies that the variation of variances could be explained by, or at least is associated with, the variation of means. Although Taylor (1961)

originally advocated the spatial TL, Taylor and Woiwod (1980) postulated a similar power-law association for both the temporal and the spatial TL; “we further conclude that the environmental effect is primarily on mean density which, in turn controls stability through behaviour, i.e. by movement”. Although this causal relationship is not denied by the results of this study, the Gompertz model shows another path that produces the temporal TL: environmental variability generates the variability of populations, and the asymmetric effect of population variability above and below the equilibrium density causes the change in the mean of population density on the natural scale.

4.3. Prevalence of the temporal TL

All simulated data sets in this study satisfied the form of the temporal TL. The model parameters used by those simulations covered most of the possible range of density dependence coefficients ($1 + a_1$ and a_2) for sustainable populations. Conversely, we conclude that most populations that obey the Gompertz model are expected to satisfy the form of the temporal TL if they are sustainable. Unsustainable populations may be members of a metapopulation in which local populations repeat extinction and colonization. Since those populations may have higher variances of population density than sustainable populations, their slopes of the temporal TL may be steeper than slopes of sustainable populations if they satisfy the temporal TL.

4.4. Range of slopes

Slopes of the temporal TL in data sets generated by Parameter combination simulation I ranged between 0.539 and 3.529 (Fig. 3A). Relatively few (7,035; 10.99%) of the time series showed $1 < b < 2$. Slopes became lower with the decrease of environmental

variability and the increase of density dependence coefficients (Table 1). Since very negative values of density dependence coefficients (a_1 and a_2) cause higher variability of population density (Royama 1992; Stenseth 1999), slopes became lower in less variable populations. In the least variable populations in simulated data sets, for which SD_j was lowest and density dependence coefficients were located on the edge of the stable region (Fig. 4), the mean slope was 1.000 (SD = 0.392, n = 36). In these simulations, very few simulated data sets had slopes smaller than 1 (0.05%). The variance and the mean of population density on the original scale increase with the increase of the variability of log populations in the Gompertz model, but the rate of increase of the variance is higher than that of mean. As a consequence, slopes become steeper than one with the increase of the variability of log populations in the Gompertz model.

The limit of the variability of populations derived from density dependence is well defined in the Gompertz model, but the variability of populations derived from environmental variability is theoretically unlimited. Therefore, it is impossible to determine the steepest possible slope of the temporal TL based on the approach of this study. In this study, we tested effects of SD in the range between 0.05 and 2.00. The range of slopes in this simulation was between 0.539 and 3.529 (Fig. 3A), and this range was observed when SD ranged between 0.05 and 0.95. When SD was equal to or higher than 1, the slopes narrowed into the range between 1.890 and 2.894.

Simulations of the Gompertz model could not explain why most observed slopes are lower than 2. However, this study clarified which parameter combinations produced $1 < b < 2$ (Fig. 3 and Appendix D). When plotting that probability for each combination of a_1 and a_2, with SD between 0.05 and 1.00, a higher probability region was found near the center of the triangle (Fig. 4), extending upper-right. Most values of a_1 and a_2 of the observed populations were included in this high-probability region. In the parameter estimates based on observed

population, the range of $1 + a_1$ was [-0.505, 0.718], and the range of a_2 was [-0.651, 0.521] (Fig. 4). Conversely, a low slope of the temporal TL indicates density dependent populations with density dependence coefficients in the right upper region of the triangle and with low environmental variability.

Taylor and Woiwod (1980) tested the temporal TL for many species of moths (n = 263), aphids (n = 97), and birds (n = 84). The mean slope (range) of the temporal TL was 1.55 (1.05–1.98) for moths, 1.99 (1.06–2.51) for aphids, and 1.30 (0.08–1.97) for birds. Additionally, Linnerud et al. (2013) reported slopes of the temporal TL for bird populations (n = 30). The mean slope (range) of the temporal TL was 1.49 (0.69–2.24). Samples of moths were collected in various environments of Great Britain and birds were observed in forests, whereas aphid samples came from open agricultural land (Taylor et al. 1980). Since an agricultural ecosystem changes greatly between cultivation and non-cultivation seasons, populations living there may repeat extinction and colonization. Since aphids inhabit those habitats, they may suffer higher environmental variability than moths, birds, and gray-sided voles. Therefore, differences in slopes of the temporal TL may reflect differences in features of population dynamics. This relationship between the temporal TL and features of population dynamics supports the suggestion of Linnerud et al. (2013) that the interspecific differences in slopes of the temporal TL can mainly be explained by effects of life history variation because environmental variability and the degree of density dependence should reflect the life history of species.

4.5. Conclusions

This study is the first to simulate extensively the effects of the model parameters (density dependence coefficients, environmental variability, and equilibrium density) of the Gompertz model on the temporal TL. Based on our simulations, we have reached the following conclusions:

1. Most closed populations that obey the Gompertz model without dispersal between populations could satisfy the form of the temporal TL if they are sustainable.

2. The variability of populations derived from environmental variability and density dependence on the log scale contributes to the temporal TL. Those factors can explain, at least partially, why $1 < b < 2$ in the temporal TL, without assuming the presence of density-dependent movement.

3. Slopes of the temporal TL become steeper (b increases) with the increase of environmental variability (SD in the Gompertz model) and with the decrease of density dependence coefficients. When environmental variability is low and density dependence is medium, the probability that TL slopes fall in $1 < b < 2$ becomes higher. But the probability is not so high, according to Figs. 3BCD: the maximum probability for $1 + a_1$ was 0.420, and the maximum for a_2 was 0.424 when SD is lower than 1.

4. The slope b may indicate features of population dynamics. Most populations that obey the Gompertz model with slopes between 1 and 2 may experience low environmental variability, and the degree of their density dependence may be intermediate.

This study did not investigate unsustainable populations and whether they are consistent with a temporal TL. Theoretical and empirical research attacking this question should contribute to understanding the range of TL slopes. In addition, extensive model analyses on the spatial TL are also promising. Parallel empirical, computational, and mathematical analyses of other nonlinear population models, such as the Ricker model commonly used in fisheries, would illuminate the robustness and generality of our conclusions here about the Gompertz model.

Acknowledgments

We thank a helpful referee for prodding us to report the mathematical analysis of the Gompertz model now reported in Appendix G. We thank the editor and both referees for helpful comments. Hayato Iijima gave T.S. helpful advice for statistical analyses. T.S. was partly supported by a Grant-in-Aid from the Japan Society for the Promotion of Science (no. 17K07552). J.E.C. acknowledges with thanks the support of U.S. National Science Foundation grant DMS-1225529 and the assistance of Roseanne K. Benjamin.

References

Anderson, A.M., Gordon, D.M., Crawley, M.J., Hassell, M.P. 1982. Variability in the abundance of animal and plant species. Nature 296, 245–248.

Bjørnstad O.N., Falck, W., Stenseth, N.C. 1995. A geographic gradient in small rodent density fluctuations: a statistical modelling approach. Proc. R. Soc. B 262, 127–133.

Bjørnstad, O.N., Stenseth, N.C., Saitoh, T. 1999. Synchrony and scaling in dynamics of voles and mice in northern Japan. Ecology 80, 622–637.

Box, G.E.P., Jenkins, G. 1970. Time Series Analysis and Control. Holden-Day, San Francisco.

Cohen, J.E., Xu, M., Schuster, W.S.F. 2013. Stochastic multiplicative population growth predicts and interprets Taylor's power law of fluctuation scaling. Proc. R. Soc. B 280, 20122955.

Cohen, J. E., Saitoh, T. 2016. Population dynamics, synchrony, and environmental quality of Hokkaido voles lead to temporal and spatial Taylor's laws. Ecology 97, 3402–3413.

Cornulier, T., Yoccoz, N.G., Bretagnolle, V., Brommer, J.E., Butet, A., Ecke, F., Elston, D.A., Framstad, E., Henttonen, H., Hörnfeldt, B., Huitu, O., Imholt, C., Ims, R.A., Jacob, J., Jedrzejewska, B., Millon, A., Petty, S.J., Pietiäinen, H., Tkadlec, E., Zub, K., Lambin,

X. 2013. Europe-wide dampening of population cycles in keystone herbivores. Science 340, 63–66.

Eisler, Z., Bartos, I., Kertész, J. 2008. Fluctuation scaling in complex systems: Taylor's law and beyond. Adv. Phys. 57, 89–142.

Hanski, I. 1982. On patterns of temporal and spatial variation in animal populations. Ann. Zool. Fenn. 19, 21–37.

Hanski, I., Woiwod, I.P. 1993. Mean-related stochasticity and population variability. Oikos 67, 29–39.

Ims, R., Andreassen, H. 2000. Spatial synchronization of vole population dynamics by predatory birds. Nature 408, 194–196.

Ishibashi, Y., Saitoh, T. 2008. Role of male-biased dispersal in inbreeding avoidance in the grey-sided vole (*Myodes rufocanus*). Mol. Ecol. 17, 4887–4896.

Kaneko, Y., Nakata, K., Saitoh, T., Stenseth, N.C., Bjørnstad, O.N. 1998. The biology of the vole *Clethrionomys rufocanu*s: a review. Res. Popul. Ecol. 40, 21-37.

Kendal, W.S. 2004. Taylor's ecological power law as a consequence of scale invariant exponential dispersion models. Ecol. Complex. 1, 193–209.

Linnerud M, Saether, B-E, Grøtan, V., Engen, S., Noble, D.G., Freckleton, R.P. 2013. Interspecific differences in stochastic population dynamics explains variation in Taylor's temporal power law. Oikos 122, 1207–1216.

Le Galliard, J-F., Remy, A., Ims, R.A., Lambin, X. 2012. Patterns and processes of dispersal behaviour in arvicoline rodents. Mol. Ecol. 21, 505–523.

Perry, J.N. 1988. Some models for spatial variability of animal species. Oikos 51, 124-130.

Reuman, D.C., Zhao, L., Sheppard, L.W., Reid, P.C., Cohen, J.E. 2017. Synchrony affects Taylor's law in theory and data. Proc. Natl. Acad. Sci. U.S.A. 183, 6788–6793.

Royama, T. 1977. Population persistence and density dependence. Ecol. Monograph 47, 1–35.

Royama, T. 1992. Analytical population dynamics. Chapman and Hall, London.

Saitoh, T., Nakatsu, A. 1997. The impact of forestry on the small rodent community of Hokkaido, Japan. Mammal Study 22, 27–38.

Saitoh, T., Stenseth, N.C., Bjørnstad, O.N. 1997. Density dependence in fluctuating grey-sided vole populations. J. Anim. Ecol. 66, 14–24.

Saitoh, T., Stenseth, N.C., Bjørnstad, O.N. 1998. Population dynamics of the vole *Clethrionomys rufocanu*s in Hokkaido, Japan. Res. Popul. Ecol. 40, 61–76.

Spiegelhalter, D.J., Thoma, A., Best, N.G., Lunn, D. 2003. WinBUGS user manual (version 1.4). MRC Biostatistics Unit, Institute of Public Health, Cambridge

Stenseth, N.C. 1999. Population cycles in voles and lemmings: density dependence and phase dependence in a stochastic world. Oikos 87, 427–461.

Stenseth, N.C., Bjørnstad, O.N., Saitoh, T. 1996. A gradient from stable to cyclic populations of *Clethrionomys rufocanus* in Hokkaido, Japan. Proc. R. Soc. B 263, 1117–1126.

Stenseth, N.C., Viljugrein, H., Saitoh, T., Hansen, T.F., Kittilsen, M.O., Bølviken, E., Glöckner, F. 2003. Seasonality, density dependence, and population cycles in Hokkaido voles. Proc. Natl. Acad. Sci. U.S.A. 100,11478–11483.

Taylor, L.R. 1961. Aggregation, variance and the mean. Nature 189:732–735.

Taylor, L.R. 1986. Synoptic dynamics, migration and the Rothamsted insect survey: Presidential Address to the British Ecological Society, December 1984. J. Anim. Ecol. 55, 1–38.

Taylor, L.R., Taylor, R. 1977. Aggregation, migration and population mechanics. Nature 265, 415–421.

Taylor, L.R., Woiwod, I.P. 1980. Temporal stability as a density dependent species characteristic. J. Anim. Ecol. 49, 209–224.

Taylor, L.R., Woiwod, I.P., Perry, J.N. 1980. Variance and the large-scale spatial stability of aphids, moths and birds. J. Anim. Ecol. 49, 831–854.

Tippett, M.K., Cohen, J.E. 2016. Tornado outbreak variability follows Taylor's power law of fluctuation scaling and increases dramatically with severity. Nature Communications 7:10668. DOI: 10.1038/ncomms10668

Table 1. Summary of the results of multiple regression analyses of the effects of environmental variability (SD) and density dependence (a_1 and a_2) on the slope b of the temporal Taylor's law using data sets generated by Parameter combination simulation I (see the main text). Although Parameter combination simulation I generated 64,000 data sets, only the 32,000 data sets with lower environmental variability [SD = 0.05-1.00] were analyzed for this table. The response variable was the slope, and explanatory variables were a_1, a_2, and SD. The full model consisted of the three variables and all their multiplicative products. The full model was selected as the best model by stepAIC. PRC = partial regression coefficient, SE = standard error of estimate.

The full model: $slope \sim a_1 + a_2 + \mathrm{SD} + a_1{:}a_2 + a_1{:}\mathrm{SD} + a_2{:}\mathrm{SD} + a_1{:}a_2{:}\mathrm{SD}$

	PRC	*SE*	*t*-value	*P*-value
Intercept	1.907	0.003	618.74	$< 2 \times 10^{-16}$
a_1	–0.512	0.006	–79.42	$< 2 \times 10^{-16}$
a_2	–0.522	0.005	–97.81	$< 2 \times 10^{-16}$
SD	0.441	0.005	81.59	$< 2 \times 10^{-16}$
$a_1{:}a_2$	–0.482	0.009	–51.01	$< 2 \times 10^{-16}$
$a_1{:}\mathrm{SD}$	0.553	0.011	48.89	$< 2 \times 10^{-16}$
$a_2{:}\mathrm{SD}$	0.492	0.009	52.57	$< 2 \times 10^{-16}$
$a_1{:}a_2{:}\mathrm{SD}$	0.464	0.017	27.96	$< 2 \times 10^{-16}$

F-statistic: 4006 on 7 and 30392 DF, *P*-value: $< 2 \times 10^{-16}$, Adjusted R^2: 0.480

Table 2. Summary of the results of multiple regression analyses of the effects of mean density (m), density dependence (a_1 and a_2), and environmental variability (SD) on the slope of the temporal Taylor's law using 512,000 data sets generated by Parameter combination simulation II (see the main text). The response variable was the slope, and the explanatory variables were m, a_1, a_2, and SD. The model consisted of the four variables and their pairwise interactions. Model selection was done by stepAIC. PRC = partial regression coefficient, SE = standard error of estimate. The primary model:

$slope \sim m + a_1 + a_2 + \mathrm{SD} + m{:}a_1 + m{:}a_2 + m{:}\mathrm{SD} + a_1{:}a_2 + a_1{:}\mathrm{SD} + a_2{:}\mathrm{SD}$

	PRC	*SE*	*t*-value	*P*-value
Intercept	1.989	0.0003	6364.8	$< 2 \times 10^{-16}$
m	7.75×10^{-7}	1.51×10^{-6}	0.513	0.608
a_1	–0.024	0.0004	–66.64	$< 2 \times 10^{-16}$
a_2	–0.022	0.0005	–45.21	$< 2 \times 10^{-16}$
SD	0.109	0.0005	211.83	$< 2 \times 10^{-16}$
$m{:}a_1$	-6.03×10^{-8}	8.43×10^{-7}	–0.072	0.943
$m{:}a_2$	4.43×10^{-7}	1.46×10^{-6}	0.303	0.762
$m{:}\mathrm{SD}$	-1.17×10^{-6}	2.39×10^{-6}	–0.491	0.623
$a_1{:}a_2$	–0.034	0.0004	–84.914	$< 2 \times 10^{-16}$
$a_1{:}\mathrm{SD}$	0.0004	0.0005	0.978	0.328
$a_2{:}\mathrm{SD}$	–0.080	0.0008	–102.23	$< 2 \times 10^{-16}$

F-statistic: 23500 on 10 and 511989 DF, *P*-value $< 2 \times 10^{-16}$, Adjusted R^2: 0.315

The model selected by AIC: $slope \sim a_1 + a_2 + \mathrm{SD} + a_1{:}a_2 + a_2{:}\mathrm{SD}$

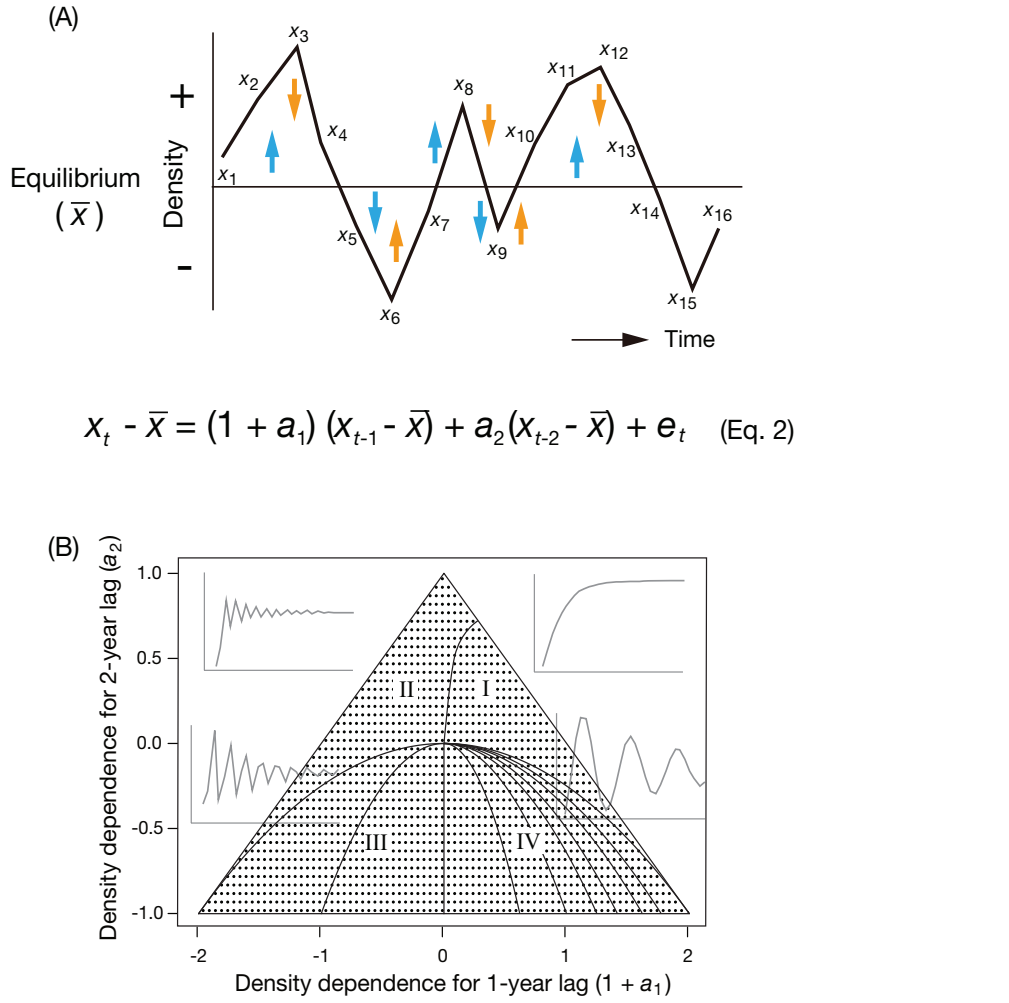

Fig. 1

Figure 1. A schema of population dynamics represented by the closed Gompertz model (Eq. 2, without dispersal between populations) and the relationship between density dependence coefficients and fluctuation patterns. x_t is the natural logarithm of the Bayesian estimate of observed density N_t. (A) In the closed Gompertz model, the equilibrium density is the mean density ($\bar{x}$) to which a population returns. A population may be forced to move from the equilibrium density by the environmental variability (arrows away from the equilibrium), but a sustainable population has a tendency to return to the equilibrium (arrows toward the equilibrium). Such a return tendency is defined as density dependence. (B) Inside the triangle, the dynamics is either point stability or damped fluctuations. A typical fluctuation pattern for each of the four parameter regions is illustrated. The fluctuations will be persistent if any level of stochasticity is present (Royama 1992). The dynamics is cyclic on the left side of $1 + a_1 = 0$ or below the semicircle (Bjørnstad et al. 1995). The lines given are contours representing the periodicity in a continuous fashion inside the semicircle from the 3-year cycle (left-most) to 10-year cycle (right-most). The outer line of the left side of the semicircle and the line separating the region I and II represent the 2-year cycle. Dots in the triangle show parameter combinations of $1 + a_1$ and a_2 that were simulated (see the main text for details). Parameters outside the triangle lead to divergence (i.e., are parameters of an unsustainable population). This figure is a modification of Fig. 3.2 in Box and Jenkins (1970, p. 59), including the same semicircle and the same numbering of quadrants.

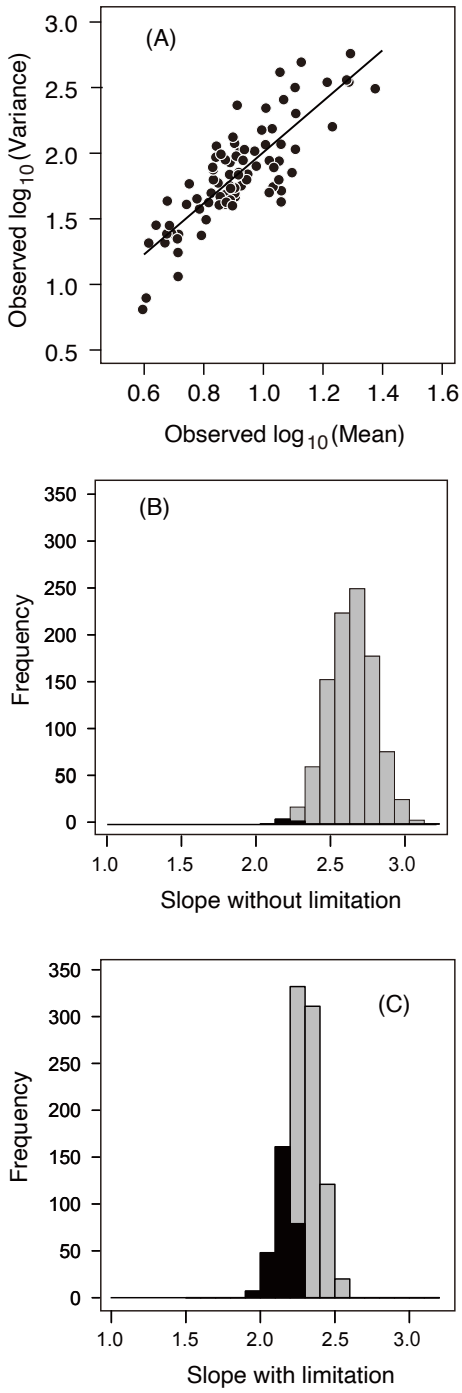

Figure 2. The temporal TL of observed populations (A) and frequency distribution of slopes in the temporal TL of simulated data sets (B) and (C). (A) A scatter plot of $\log_{10}$(temporal variance) as a function of $\log_{10}$(temporal mean) for observed data sets of the $\log_{10}$ Bayesian estimate of population density $N_{t,j}$ of 85 gray-sided vole populations in Hokkaido, Japan in t = 1962, …, 1992. The solid line is the ordinary least-squares linear regression (OLS) of $\log_{10}$(variance) against $\log_{10}$(mean). (B) Frequency distribution of slopes in the temporal TL for 1,000 simulated data sets generated by Fundamental simulation I, accepting all simulated population densities generated by the model. (C) Frequency distribution of slopes in the temporal TL for 1,000 simulated data sets generated by Fundamental simulation II, modifying unrealistically high values. A solid black area indicates the simulated slopes that fell in the 95% CI of the observed slopes.

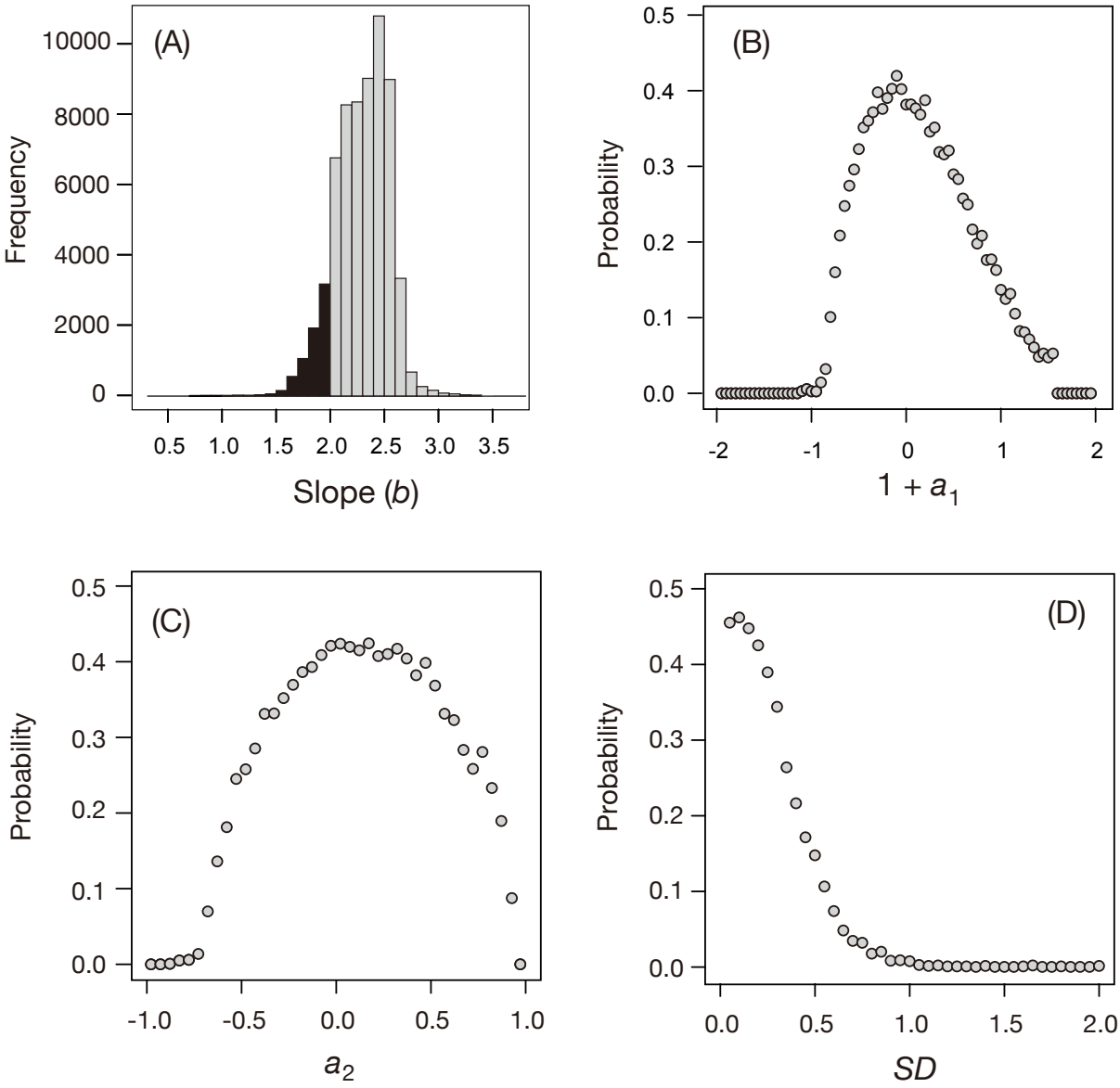

Figure 3. Frequency distribution of slopes b of the temporal TL and the probability that each of the three model parameters (a_1, a_2 and SD) of the Gompertz model produced slopes of the temporal TL in $1 < b < 2$ in time series generated by Parameter combination simulation I (see the main text for details). Each dataset consisted of 85 simulated populations over 31 years. (A) Frequency distribution of 64,000 values of slope b (range: 0.539 to 3.529). A solid black area indicates the simulated slopes in $1 < b < 2$. (B) Data sets generated with SD between 0.05 and 0.95 (n = 32,000) in (B) and (C) covered almost all variation of slopes. The probability that a slope fell in $1 < b < 2$ for 79 values of the density dependence coefficient with 1-year lag ($1 + a_1$) between –2 and +2 (n = 32,000) peaked near ($1 + a_1$) = 0. (C) The probability that a slope fell in $1 < b < 2$ for 40 values of the density dependence coefficient with 2-year lag (a_2) between –1 and +1 (n = 32,000) peaked near $a_2 = 0$. (D) The probability that a slope fell in $1 < b < 2$ for 40 values of the environmental variability parameter (SD) covering the full range of SD between 0.05 and 2.00 (n = 64,000) peaked near the smallest simulated value of SD.

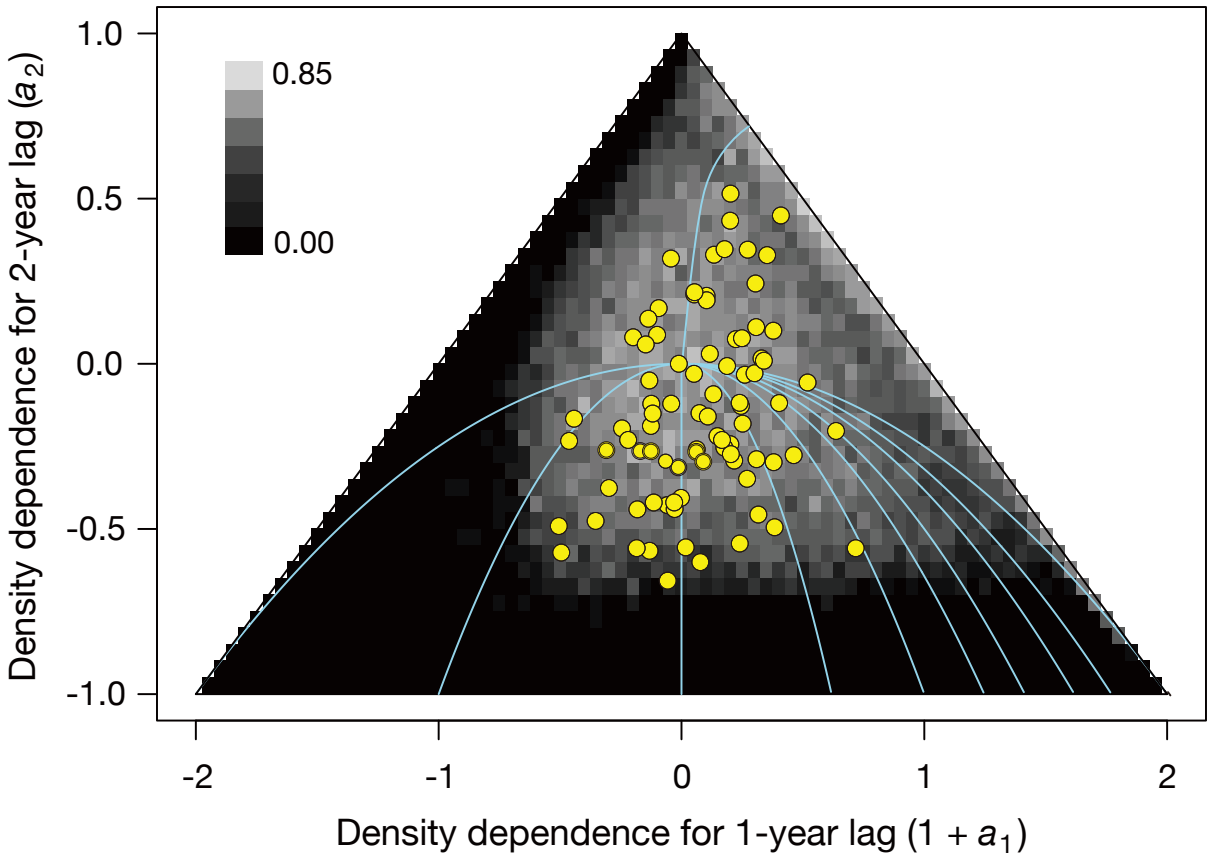

Figure 4. The relationship between slope (b) and density dependent coefficients (a_1 and a_2) in Parameter combination simulation I. The shading of each cell indicates the probability that simulated data sets had slope $1 < b < 2$ for each combination of density dependent coefficients (a_1 and a_2) within the triangle in the range of SD between 0 and 1. Lighter shading shows higher probability. Observed populations of the Hokkaido vole are illustrated by open yellow circles ($n = 85$). They are scattered in the lighter area.